Impact of CAV Parameters and Intersection Complexity on Stop-Controlled Intersection Efficiency: A Simulation Study

Atasi Roy Malakar

Department of Civil and Environmental Engineering
University of Wisconsin-Madison

May 3, 2025

Abstract

Intersections, particularly stop-controlled ones, are significant bottlenecks in urban transportation networks, contributing to delays, reduced efficiency, and safety concerns. Connected and Automated Vehicles (CAVs) offer potential improvements through optimized operational parameters (e.g., reduced headways, higher speeds) and advanced coordination capabilities. This report presents a simulation model developed in MATLAB to analyze and quantify the potential throughput efficiency gains at a two-approach, multi-lane stop-controlled intersection by comparing scenarios using CAV operational parameters against those using Human-Driven Vehicle (HDV) parameters. The model implements a *block-priority scheduling logic*: vehicles arriving closely together from the same approach are grouped into blocks, and the block, whose first vehicle arrives earliest at the control point, generally gains priority to proceed. A key feature is a processing algorithm that enforces switching time headways between blocks from conflicting approaches and re-validates car-following headways within lanes after potential adjustments, ensuring conflict-free operation. A single-run simulation provides a detailed look at the model's mechanics and scheduling adjustments using illustrative parameters justified by literature ranges. Furthermore, a multi-trial analysis using randomized intersection configurations explores the relationship between intersection complexity (quantified as the product of lanes per approach) and the percentage efficiency gain offered by CAV parameters. Results indicate substantial efficiency improvements with CAV parameters, though the magnitude of the gain varies with intersection complexity and other stochastic factors. The study highlights the importance of detailed modeling for unsignalized intersections and provides a quantitative baseline for evaluating CAV impacts within traditional control paradigms, acknowledges model limitations, and outlines directions for future research. The simulation code is publicly available on GitHub.

Contents

1 Introduction

Intersections form critical junctures in road networks, frequently functioning as significant bottlenecks that impede traffic flow and compromise safety [32]. Unsignalized intersections, including stop-controlled ones, are particularly challenging, contributing substantially to traffic delays, fuel consumption, emissions, and accidents [21, 3]. Traffic congestion arising from intersection inefficiencies imposes significant economic costs due to lost productivity and wasted fuel [16]. Traditional intersection control methods, like fixed stop signs or basic signal timings, struggle to adapt efficiently to varying traffic demands and the inherent limitations of human drivers [8]. Enhancing intersection efficiency, therefore, offers considerable advantages in terms of reduced travel times, lower environmental impact, and potentially improved safety [2, 40].

Responding to these challenges, the emergence of Connected and Automated Vehicles (CAVs) presents a significant opportunity to mitigate these issues [35]. Equipped with advanced sensing, communication (Vehicle to Everything, V2X), and control capabilities, CAVs can operate with optimized parameters (shorter headways, faster reaction times, potentially higher speeds) and enable sophisticated coordination strategies [11, 23].

Much research focuses on advanced CAV applications at intersections, such as reservation-based Autonomous Intersection Management (AIM) [7, 37, 18], trajectory optimization for signalized [14, 40] or signal-free crossings [31, 13], platoon control [37, 4, 24], and complex scheduling algorithms using game theory [15, 38], machine learning [10, 33], quantum computing [26], or edge computing [28]. These approaches often demonstrate substantial theoretical benefits in efficiency and safety [19].

However, the transition to fully automated, coordinated systems will be gradual, involving extended periods of mixed traffic where CAVs and conventional Human-driven Vehicles (HDVs) coexist, often navigating infrastructure designed around traditional control methods like stop signs or traffic signals [21, 19, 27, 40]. Safety in these mixed environments is a key concern, as conflicting driving behaviors between CAVs and HDVs can arise [21]. Understanding these baseline parameter-driven gains is crucial for developing realistic deployment timelines and assessing the initial return on investment for CAV technology integration into existing infrastructure. Conversely, without quantifying these fundamental improvements offered simply by CAV parameters, planning efforts may overestimate the immediate need for complex cooperative infrastructure or misjudge the inherent capabilities CAVs bring even to legacy systems like stop-controlled intersections.

Some studies compare CAV performance at different intersection types [35] or assess specific Vehicle to Infrastructure (V2I) applications like Stop Sign Gap Assist (SSGA) [3]. However, there remains a need for detailed simulation comparing HDV and CAV parameters under rule-based stop control, especially in multi-lane configurations requiring robust conflict resolution.

This study attempts to fill this gap by developing and utilizing a detailed simulation model in MATLAB that compares HDV and CAV performance under an identical, rigorously enforced stop-sign protocol using *approach-based block-priority scheduling*. The novelty lies in quantifying the efficiency gains attributable purely to differences in vehicle performance parameters while employing a processing algorithm to ensure conflict-free scheduling in a multi-lane environment based on this priority logic, contrasting with both simple FIFO [18, 34] and complex optimization approaches [28, 31, 33]. The central problem addressed is the quantitative comparison of operational efficiency (throughput efficiency relative to theoretical saturation flow, average vehicle delay) at a multi-lane, two-approach stop-controlled intersection when operated by HDVs versus CAVs, using distinct but representative parameter sets.

The simulation determines departure order based on a block-priority scheduling logic: groups of vehicles arriving closely from the same approach are considered, and the block whose first vehicle

arrives earliest generally proceeds first. It calculates potential stop times incorporating segment travel time (δ) and car-following headways ($\tau_{F,mod}$). A detailed processing algorithm analyzes the schedule, identifies vehicle blocks, rigorously enforces switching headways ($\tau_{S,mod}$) between conflicting blocks, adjusts subsequent vehicle stop/departure times to account for cascading delays, and resolving potential conflicts while adhering to the block-priority principle. The comparison isolates the impact of using CAV-specific parameters versus HDV parameters within this controlled framework. The simulation outputs detailed vehicle trajectories and performance metrics, facilitating direct comparison, visualization, and analysis of efficiency gains versus intersection complexity.

This report is structured sequentially: Section 2 reviews relevant literature, Section 3 details the simulation methodology, and Section 4 presents the simulation results. These results are further analyzed in Section 5. Subsequently, Section 6 addresses the study's limitations, Section 7 provides the concluding remarks, and Section 8 outlines practical implications and future research directions. The report concludes with Appendix A, which lists all cited references.

2 Literature Review

The study of intersection performance and the potential impact of CAVs builds upon decades of research in traffic flow theory, driver behavior modeling, and automated vehicle control. This review covers modeling approaches for HDVs and CAVs at intersections, focusing on unsignalized scenarios, scheduling/coordination strategies, and mixed traffic conditions relevant to this study.

2.1 HDV Intersection Modeling and Capacity Analysis

Traditional analysis of stop-controlled intersections often relies on gap acceptance models and queuing theory to estimate capacity and delay for HDVs. The Highway Capacity Manual (HCM) provides standardized methodologies based on critical gap (t_c) and follow-up time (t_f) parameters. Critical gap values typically range from 6-8 seconds for stop-controlled approaches, depending on the movement type and major road characteristics [9, 6, 36]. Follow-up times are generally shorter, often around 3-4 seconds [9]. Accurate modeling of driver gap acceptance behavior, which exhibits considerable variability, is critical, as highlighted by Arafat et al. (2021), who demonstrated that using default simulation parameters instead of calibrated, distribution-based gap acceptance models can significantly overestimate capacity at two-way stop-controlled (TWSC) intersections [3]. Microscopic simulation models (e.g., VISSIM, SUMO) are widely used to capture more detailed interactions, often incorporating car-following models like Gipps or the Intelligent Driver Model (IDM) [21, 19]. Studies using naturalistic driving data suggest average car-following headways (τ_F) are often in the range of 1.5-2.0 seconds, but can extend to 4 seconds or more under certain conditions or for more cautious drivers [39, 1].

2.2 CAV Intersection Strategies and Scheduling

Building upon this HDV modeling foundation, the advent of CAVs has led research to intensely focus on novel intersection management strategies aiming for higher efficiency and safety than traditional control. These range from rule-based systems to complex optimization frameworks:

- **Rule-Based and Priority Systems:** The simplest rule is First-In-First-Out (FIFO), often used as a baseline [18, 33]. Soomro et al. (2024) combined FIFO with a priority queue to manage emergency CAVs [34]. However, pure FIFO can be inefficient [18] particularly in multi-lane settings where it doesn't inherently coordinate across lanes from the same approach, motivating approaches like the block-priority logic used here. Variations include

platoon ordering based on turns before reservation [37] or using priority trees considering conflicts, waiting times, and arrival times [29]. Shao et al. (2023) used multi-lane queue models and a cost function incorporating efficiency, waiting time, and static priority to determine passing sequences [32]. The block-priority approach in the current study fits within this category, prioritizing groups from the same approach based on earliest readiness.

- **Reservation-Based Systems:** Autonomous Intersection Management (AIM) allows vehicles to reserve time-space slots through the intersection, potentially eliminating stops [7]. While highly efficient, these systems typically require significant communication and coordination infrastructure, contrasting with our study's focus on performance improvements within the existing stop-control paradigm. Various protocols exist, including batch reservations and token-based systems [32]. Tunc et al. (2024) combined reservation systems with platoon ordering [37].

- **Optimization-Based Scheduling:** Many approaches formulate scheduling as an optimization problem. Jin et al. (2012) showed optimal scheduling significantly outperforms FIFO [18]. These optimization approaches often seek system-wide optima in signal-free environments [28, 31], whereas our work analyzes efficiency under a predefined, sub-optimal but potentially more readily implementable rule-based protocol.

  Various techniques are employed, including Mixed Integer Linear/Non-Linear Programming (MILP/MINLP) [40], convex optimal control for trajectory planning [31], game theory to model interactions and resolve conflicts [15, 38], machine learning (e.g., Reinforcement Learning for car-following [10] or Q-learning for platoon control [24]), advanced search methods like Neural Monte Carlo Tree Search [33], and even exploring quantum annealing for the underlying combinatorial optimization problems (often Minimum Clique Cover on conflict graphs) [26]. Lu et al. (2024) used edge computing to solve an Absolute Value Programming formulation for optimal entry times [28]. Gu et al. (2024) used an IoT framework with Petri nets [13]. These methods often target signal-free environments and aim for system optimality but face computational challenges [33].

- **Distributed vs. Centralized Control:** While many systems assume a central intersection manager (like AIM or optimization solvers), distributed approaches using Vehicle to Vehicle (V2V) communication for conflict resolution are also researched [25], potentially offering more scalability.

2.3 Mixed Traffic Analysis

The transition period will involve mixed traffic streams of HDVs and CAVs, presenting unique challenges and opportunities [21, 40, 2]. Modeling these interactions accurately is crucial.

- **Capacity and Efficiency:** Ghiasi et al. (2017) provided a foundational review of mixed traffic headways (reporting CAV-CAV τ_F potentially as low as 0.3-0.6s, and using means around 0.85s for CAV-CAV and 1.1-1.5s for mixed headways in examples) and analyzed freeway capacity using Markov chains [11]. Li et al. (2019) extended gap acceptance theory for unsignalized intersection capacity with mixed flows and platoons [23]. Tafidis et al. (2019) simulated CAV introduction and found performance impacts varied by intersection control type, with uncontrolled intersections showing greater relative improvements [35]. Studies on freeways suggest capacity generally increases with CAV MPR, but the relationship can be complex [20]. Chen et al. (2022) developed a cooperation strategy specifically for multi-lane unsignalized intersections with mixed CAVs and connected HDVs, focusing on platoon

formation to improve flow [4]. Capacity analyses often explore CAV headways in the 0.5s to 2.0s range depending on assumed control strategy and aggression.

- **Safety:** Karbasi & O'Hern (2022) used SUMO and surrogate safety measures (TTC) to assess safety at signalized and unsignalized intersections, finding CAVs (especially with CACC) generally reduce conflicts, but effects depend on MPR [19].

  Lee et al. (2024) used driving simulators and VISSIM, identifying unsignalized turns as particularly challenging in mixed traffic, with safety varying non-monotonically with MPR depending on the specific conflict type and driving behavior models used (W99 vs IDM) [21].

- **Signalized Intersection Control:** Significant research exists on optimizing control for mixed traffic at signalized intersections. Zou et al. (2024) proposed a hierarchical framework combining platoon-based MILP for signal/arrival time optimization with DMPC for trajectory control [40]. Ahmad et al. (2024) developed an eco-driving framework using ML for signal optimization and decentralized control for CAV speed adjustment [2]. Liu et al. (2024) researched speed guidance strategies considering HDV uncertainty [27]. Guo & Ma (2021) used DRL for signal optimization combined with TP3 for trajectory control, including LSTM for HDV state estimation [14]. While focused on signalized intersections, these studies address key mixed-traffic issues like HDV uncertainty and platoon management.

2.4 Gap Addressed by This Study

While CAV coordination is widely studied [40, 2, 27, 14, 31, 33, 26, 28, 13, 23], the fundamental efficiency impact of CAV operational parameters alone within traditional, rule-based, multi-lane stop-controlled intersections is less understood. This study quantifies this specific baseline improvement potential. We employ a block-priority scheduling logic [30], distinct from both FIFO [18] or complex optimization [32, 29], and uniquely incorporate an explicit post-processing step for multi-lane conflict resolution to enforce headways -addressing realistic geometric complexities often simplified elsewhere. By isolating parameter effects (headways, speed, etc.) for CAVs and HDVs under this protocol, we provide a quantitative benchmark for parameter-driven benefits at conventional multi-lane stop signs, bridging the gap between basic models and fully cooperative systems.

3 Methodology

This study employs a microscopic simulation approach implemented in MATLAB to model and compare the performance of HDVs and CAVs at a multi-lane, two-approach, stop-controlled intersection. The overall simulation logic follows the process outlined in Figure 1. It begins with user inputs and parameter calculations, generates stochastic vehicle arrivals, and then schedules vehicles based on a block-priority principle. Groups of vehicles arriving closely from the same approach form blocks, and the block arriving earliest and ready earliest at the stop line generally proceeds first. A crucial processing phase refines the schedule generated by this priority logic to resolve potential conflicts and ensure headway compliance before final performance metrics are calculated and results visualized. The core methodology involves the following key steps:

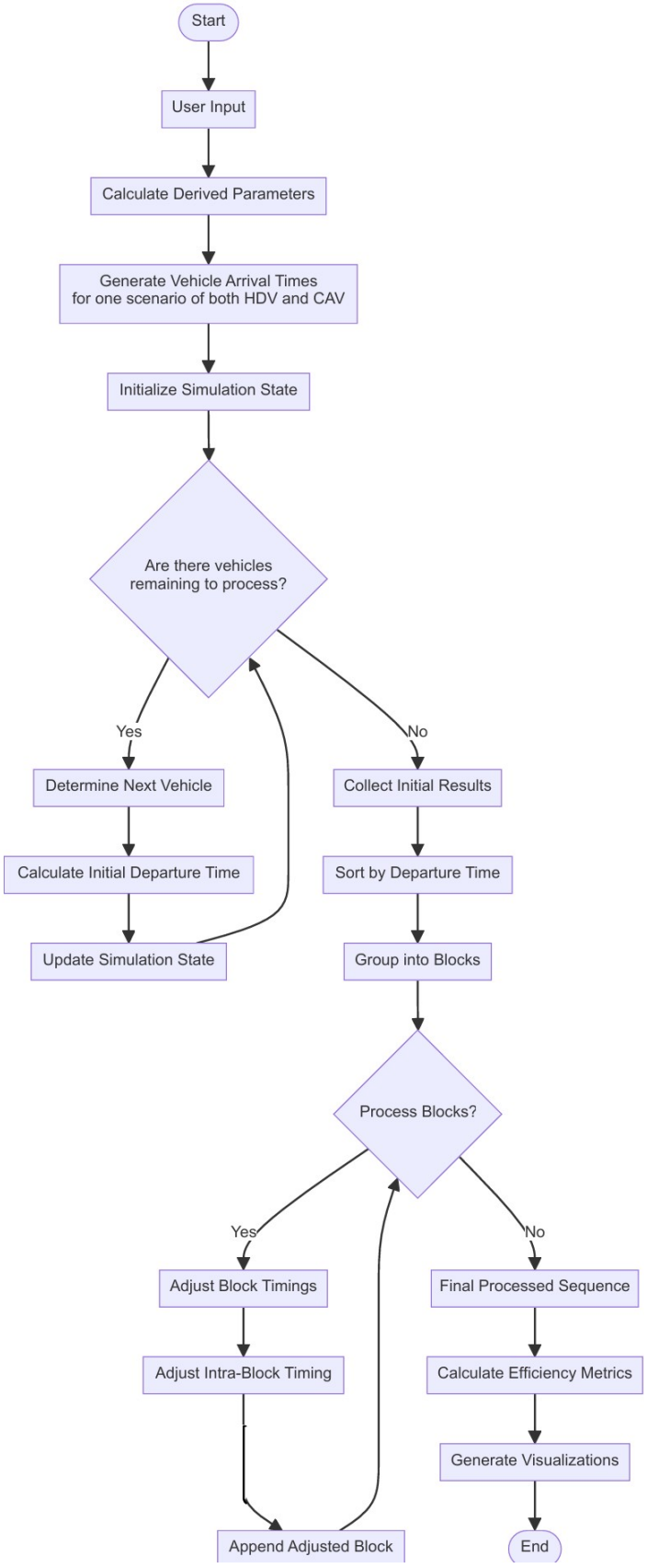

Figure 1: Overall simulation logic flowchart, outlining block identification, priority scheduling, and headway enforcement steps.

3.1 Simulation Environment

The simulation models a four-legged stop-controlled intersection where two one-way approaches cross at right angles. Each approach consists of one or more lanes dedicated to through traffic only. Vehicles are required to come to a complete stop at the designated stop line before entering the intersection box. This setup functions similarly to an all-way stop-controlled intersection, where traffic from all modeled approaches must stop before proceeding, typically following a priority rule like the block-priority logic described later.

3.2 Intersection and Vehicle Parameters

This step corresponds to the "User Input" and "Calculate Derived Parameters" stages in the flowchart (Figure 1). Several physical and operational parameters define the simulation environment:

- **Constants:**

  The following fixed physical parameters define the simulation environment:

  - A **standard lane width** (`lane_width`) of 12 ft is assumed, reflecting AASHTO's recommendation for relevant road types [41].
  - A **stop line setback** (`offset`) of 4 ft defines the distance from the physical intersection box edge to the required stopping point.
  - An **approach segment length** (`L`) of 100 ft marks the starting point from which vehicles travel towards the intersection.
  - **Uniform vehicle dimensions** (`veh_length` = 14 ft, `veh_width` = 6 ft) are used for all vehicles, representing the approximate size of a typical compact passenger car such as a Volkswagen Golf [42].

- **Geometric Configuration and Demand:** These parameters define the intersection layout and traffic volume. For single illustrative runs, specific values are set (by user or default), while they are randomized in the multi-run analysis:

  - Number of approaches (N_{app}): Fixed at 2 for this study.
  - Lanes per approach ($N_{lanes,p}$): Defines the number of lanes for approach p.
  - Vehicles per lane ($N_{veh,p,l}$): Specifies the initial vehicle count for each lane l on approach p.

- **Calculated Intersection Geometry:** The dimensions of the intersection conflict box are derived from the lane configuration and offset:

  - Box Length (`box_length`): Calculated as $\texttt{lane\_width} \times N_{lanes,2} + 2 \times \texttt{offset}$. (Assumes Approach 2 dictates length based on its lanes crossing Approach 1).
  - Box Width (`box_width`): Calculated as $\texttt{lane\_width} \times N_{lanes,1} + 2 \times \texttt{offset}$. (Assumes Approach 1 dictates width).

- **Operational Parameters:** These define vehicle behavior and arrivals, with distinct values typically used for HDV and CAV scenarios:

  - Speed (v): Posted speed, used for arrival and constant departure phases in this model (ft/s).

- Deceleration (a_{min}): Maximum desired deceleration rate (ft/s^2, negative value).
- Acceleration (a_{max}): Maximum desired acceleration rate (ft/s^2, currently only for visualization/future model extension).
- Switching Time Headway (τ_S): Minimum desired time gap between vehicles from conflicting approaches (s).
- Car-Following Time Headway (τ_F): Minimum desired time gap between consecutive vehicles in the same lane (s).
- Arrival Rate (λ): Parameter for the Poisson arrival process (average rate per approach, veh/s).

The specific parameter values are detailed in the Notation Summary (Table 1) and in the Results section (Table 2). The fundamental scheduling logic for processing vehicles at a stop line was adapted from concepts presented in the Connected and Automated Transportation Systems course (CIVENGR 570, Spring 2025) at the University of Wisconsin-Madison [30], significantly extended here to handle multi-lane scenarios and implement the block-priority scheduling with conflict resolution. The simulation code implementing this methodology is publicly available on GitHub [12].

3.3 Headway Modifications and Safety Constraints

User-input headways (τ_F, τ_S) represent desired minimums. The simulation enforces physical constraints by calculating and using modified headways ($\tau_{F,mod}, \tau_{S,mod}$) internally:

- **Modified Car-Following Headway ($\tau_{F,mod}$):** Ensures minimum physical separation. $\tau_{F,mod} = \max(\tau_F, 1.5 \times l_{veh}/v)$. (Caution: Input τ_F below this physical limit might be overridden by the simulation to ensure safety).
- **Modified Switching Headway ($\tau_{S,mod}$):** Ensures time to clear intersection box. $\tau_{S,mod} = \max(\tau_S, (l_{veh} + \max(b_L, b_W))/v)$. (Caution: Input τ_S below this physical limit might be overridden by the simulation to ensure safety).

The scheduling logic respects these physical minimums, and the fundamental scheduling logic as well as the block merging process explicitly enforces the modified values, if necessary, before applying necessary shifts.

3.4 Vehicle Arrival Generation

Following parameter definition, vehicle arrivals are generated stochastically ("Generate Vehicle Arrival Times" in Figure 1). For each approach p, vehicle arrival times t_{pi}^- at the start of segment L are determined as follows:

1. Determine total vehicles $N_{veh,p}$ by summing 'vehicle_countsp' across its lanes.
2. Generate $N_{veh,p}$ inter-arrival times from an exponential distribution with rate λ.
3. Enforce a minimum physical gap ('min_gap_time' $\approx 1.5 \times l_{veh}/v + v/(-2a_{min})$) between arrivals.
4. Calculate absolute arrival times t_{pi}^- using 'cumsum'.
5. Randomly assign vehicles to lanes within the approach using 'randperm', preserving per-lane counts.
6. Sort final arrival data by t_{pi}^-.

3.5 Core Simulation Process

This section details the core simulation process in the first script named 'CODE.m', combining elements shown from "Initialize Simulation State" through "Append Adjusted Block" in Figure 1. The simulation schedules vehicle departures based on prioritizing blocks of closely arriving vehicles from the same approach.

1. **Segment Travel & Stop Time (δ):** Calculate time from segment start to stop: $\delta = L/v + v/(-2 \times a_{min})$.

2. **Determine Potential Stopping Time (t_{pi}^0):** For the next candidate vehicle i in lane l of approach p, calculate its earliest possible stop time considering arrival and intra-lane car-following: $t_{pi}^0 = \max(t_{pi}^- + \delta, t_{p,l,prev}^+ + \tau_{F,mod})$, where $t_{p,l,prev}^+$ is the departure of the previous vehicle *in the same lane*, and $\tau_{F,mod}$ is the modified car-following headway (Section 3.3).

3. **Identify Next Ready Vehicle/Block:** Globally identify the vehicle (across all approach queues) that has the minimum potential stopping time t_{pi}^0. This vehicle represents the start of the next potential block to be processed, establishing the priority based on the earliest ready block.

4. **Generate Initial Sequence Order:** Iteratively repeat steps 2-3 to determine the order in which vehicles become ready at the stop line, generating a preliminary sequence. Calculate initial departure times t_{pi}^+ based on t_{pi}^0 and the switching headway $\tau_{S,mod}$ relative to the departure time of the *absolute last vehicle* processed ($t_{p_{prev},last}^+$).

5. **Group into Blocks:** Process the initial sequence (sorted by initial departure time t_{init}^+) to group vehicles into "blocks". A new block begins whenever the current vehicle is from a different approach than the previous vehicle, OR if it's from the same approach but the time gap since the previous vehicle's departure is $\geq \tau_{S,mod}$. Vehicles within a block are from the same approach and initially scheduled closely.

6. **Merge Blocks and Enforce Headways:** Sequentially merge these blocks into a final schedule ('final_block'), applying conflict resolution:

   - **Switching Headway ($\tau_{S,mod}$) Enforcement (Inter-Block)**: When merging a block ('curr_block') that starts with a conflicting approach relative to the last vehicle in the currently merged 'final_block', ensure the first departure t^+ in 'curr_block' is $\geq$ last departure + $\tau_{S,mod}$. If an adjustment is needed, shift the departure times t^+ of vehicles in 'curr_block' forward accordingly.
   - **Car-Following ($\tau_{F,mod}$) Re-validation (Inter- and Intra-Block)**: After any potential $\tau_{S,mod}$ shift, rigorously re-check the car-following headway $\tau_{F,mod}$ for *each vehicle* within the 'curr_block'. Check against the immediate preceding vehicle, if any, from the same lane either already in the merged 'final_block', or within the 'curr_block'. If a violation is found, adjust the vehicle's stop time t^0 upwards and update its departure time $t^+ = \max(t^+, t^0)$ to satisfy $\tau_{F,mod}$, propagating necessary delays.
   - **Append:** Append the adjusted 'curr_block' to 'final_block'.

7. **Final Sort:** Sort the completed 'final_block' by the final departure time t_{final}^+.

This integrated process ensures the final schedule reflects the block-priority principle, adheres to both car-following and switching headways, and resolves multi-lane conflicts. Note: in some scenarios where no conflict arises, the post-processing step does not result in any change in the initially generated sequence.

3.6 HDV vs. CAV Scenarios

The core comparison runs the simulation twice with different parameter sets:

- **HDV Parameters:** Longer headways ($\tau_{F\_human}, \tau_{S\_human}$), potentially lower speeds (v_{human}), lower acceleration/deceleration ($a_{max\_human}, a_{min\_human}$), potentially different arrival rates (λ_{human}). Values are often informed by literature like [11, 1, 9].
- **CAV Parameters:** Shorter headways ($\tau_{F\_cav}, \tau_{S\_cav}$), potentially higher speeds (v_{cav}), higher acceleration/deceleration (a_{max_cav}, a_{min_cav}), potentially different arrival rates (λ_{cav}). (Note: τ_{F_cav} here is conservative, not representing ultra-short platooning headways). Values are often informed by literature like [11].

The number of lanes and vehicles are kept identical for a fair comparison based on operational parameters.

3.7 Performance Metrics

After obtaining the final sequence, performance metrics are calculated ("Calculate Efficiency Metrics" in Figure 1).

1. **Throughput Efficiency (%):** Calculated by the `compute_efficiency` function.
   - Actual Throughput = Total Vehicles ÷ (Last Departure Time − First Departure Time).
   - Theoretical Maximum Throughput ≈ $S_0 \times \max(N_{\text{lanes},p})$, where S_0 is the standard saturation flow rate (e.g., 1800 veh/hr/lane from American Association of State Highway and Transportation Officials, AASHTO). This represents idealized flow capacity.
   - Efficiency = (Actual Throughput ÷ Theoretical Maximum) ×100.
2. **Average Vehicle Delay (s):** Computed as the mean of $(t^{+}_{\text{final}} - t^{0}_{\text{final}})$ across all vehicles. This represents the average wait time at the stop line. Results are visualized in Figure 2.

Visualization (snapshot from video generated by code) of the simulation run comparison Figure 3 is also generated.

3.8 Multi-Run Simulation for Conflict Point Analysis

This analysis uses the second script 'trial_submission.m' to explore sensitivity. It performs multiple trials (e.g., 50,000):

1. Randomize geometry: Generate random $N_{lanes,p}$ (1 to 20) and $N_{veh,p,l}$ (5 to 100).
2. Run HDV and CAV simulations using **fixed default operational parameters** coded in the script (HDV: v=45 ft/s, a_{min}=-5 ft/s^2, a_{max}=6.5 ft/s^2, τ_S=2.5 s, τ_F=2 s, λ=0.3; CAV: v=60 ft/s, a_{min}=-15 ft/s^2, a_{max}=10 ft/s^2, τ_S=0.8 s, τ_F=0.6 s, λ=0.7). Note these differ from the single illustrative run parameters.

Default Parameter Justification: The default parameters used in these multi-run simulations represent typical or literature-informed values selected for comparative analysis across a wide range of scenarios. The specific values and their justifications are:

- **HDV Parameters:** These values represent typical human driving behavior under stop control:
  - Speed (v_{HDV}): Set to 45 ft/s ($\approx$ 30 mph), reflecting a common arterial/collector road speed limit.
  - Car-Following Headway ($\tau_{F,HDV}$): Set to 2.0 s. This aligns with frequently cited average observed headways [39, 1].
  - Switching Headway ($\tau_{S,HDV}$): Set to 2.5 s. This represents efficient HDV operation at a stop sign, chosen closer to typical follow-up times (t_f) than potentially longer critical gaps (t_c) found in some HCM methodologies [9, 36].
  - Acceleration/Deceleration ($a_{max,HDV} = 6.5$ ft/s^2, $a_{min,HDV} = -5$ ft/s^2): Typical values for conventional HDVs.
- **CAV Parameters:** These values represent potentially more aggressive but feasible automated operation:
  - Speed (v_{CAV}): Set to 60 ft/s ($\approx$ 41 mph), reflecting potential operational speed improvements.
  - Car-Following Headway ($\tau_{F,CAV}$): Set to 0.6 s. This represents aggressive, highly efficient independent (non-platooning) automated operation, consistent with values explored in simulation studies [11].
  - Switching Headway ($\tau_{S,CAV}$): Set to 0.8 s. This also assumes efficient automated operation, informed by simulation values [11].
  - Acceleration/Deceleration ($a_{max,CAV} = 10$ ft/s^2, $a_{min,CAV} = -15$ ft/s^2): Reflects potentially higher capabilities of automated systems.
- **Arrival Rates (λ):** These were selected to explore performance under varying demand levels across the randomized geometries:
  - HDV Arrival Rate (λ_{HDV}): 0.3 veh/s/approach (1080 veh/hr/approach), representing moderate-to-high demand.
  - CAV Arrival Rate (λ_{CAV}): 0.7 veh/s/approach (2520 veh/hr/approach), representing very high demand to test the system under load.

3. Calculate efficiencies E_{HDV}, E_{CAV}.
4. Calculate Percentage Efficiency Gain $= ((E_{CAV} - E_{HDV})/E_{HDV}) \times 100$.
5. Calculate Conflict Points $CP = N_{lanes,1} \times N_{lanes,2}$.
6. Log $(CP, Gain)$ for each trial.
7. Generate scatter plot (Figure 4) and save data.

Aggregate results are then analyzed.

3.9 Notation Summary

Table 1 summarizes the key symbols and abbreviations used throughout this report for clarity.

Table 1: Table of Notation

Symbol	Description
N_{app}	Number of approaches (fixed at 2 for this study)
p	Approach index, $p \in \{1(\text{Approach A}), 2(\text{Approach B})\}$
$N_{lanes,p}$	Number of lanes for approach p
l	Lane index within an approach, $l \in \{1, ..., N_{lanes,p}\}$
$N_{veh,p,l}$	Number of vehicles initially assigned to lane l of approach p
i	Vehicle sequence number within a specific lane queue (based on arrival time t^-)
L	Length of the approach segment before the stop line (ft)
l_{veh}	Length of each vehicle (assumed uniform) (ft)
w_{veh}	Width of each vehicle (assumed uniform) (ft)
w_{lane}	Width of each lane (ft)
$offset$	Setback distance of stop line from the physical start of the intersection box (ft)
v	Arrival speed at start of segment L; posted speed (ft/s)
a_{min}	Maximum desired deceleration rate (ft/s^2, typically negative)
a_{max}	Maximum desired acceleration rate (ft/s^2) (This was not used in the current model but included for completeness/future work)
τ_F	User defined minimum desired car-following time headway between 2 consecutive vehicles in the same lane (s)
τ_S	User defined minimum desired switching time headway between approaches (s)
λ	Parameter for Poisson arrival process (average arrival rate per approach) (veh/s)
δ	Time for vehicle to travel segment L and stop (s)
b_L, b_W	Length and width of the intersection conflict box (ft)
$\tau_{F,mod}$	Modified (if necessary) car-following headway used in simulation (enforces physical minimum) (s)
$\tau_{S,mod}$	Modified (if necessary) switching headway used in simulation (enforces physical minimum) (s)
t^-	Absolute arrival time of a vehicle at the start of segment L (s)
t^0	Time a vehicle stops at the stop line (s) (t^0_{init}: potential value, t^0_{final}: after adjustments)
t^+	Time a vehicle departs from the stop line (s) (t^+_{init}: initial schedule value, t^+_{final}: after adjustments)
last_depart_lane(p, l)	Time the last vehicle departed from lane l, approach p (s)
last_departure(p)	Time the last vehicle departed from approach p (s)
p_{prev}	Index of the approach from which the globally last vehicle departed
Block	A group of consecutive vehicles from the same approach scheduled closely together
T_{total}	Total simulation time span (first departure to last departure) (s)

Continued on next page

Table 1 – continued from previous page

Symbol	Description
$N_{total\_vehicles}$	Total number of vehicles processed in a run
$Throughput_{actual}$	Actual simulated throughput (veh/s)
S_0	Assumed saturation flow rate per lane (veh/s/lane)
$Throughput_{max}$	Estimated theoretical maximum throughput for the geometry (veh/s)
$Efficiency$	Throughput Efficiency (%)
CP	Conflict Points ($N_{lanes,1} \times N_{lanes,2}$), metric for intersection complexity
$Gain$	Percentage Efficiency Gain (CAV vs HDV) (%)
HDV	Human-Driven Vehicle
CAV	Connected and Automated Vehicle
FIFO	First-In-First-Out
V2X	Vehicle-to-Everything Communication
MATLAB	Matrix Laboratory (Software Environment)
GUI	Graphical User Interface
CSV	Comma-Separated Values (File Format)
HCM	Highway Capacity Manual
IDM	Intelligent Driver Model (a car-following model)
CACC	Cooperative Adaptive Cruise Control
ACC	Adaptive Cruise Control
SUMO	Simulation of Urban Mobility
VISSIM	Verkehr In Städten SIMulationsmodell (Traffic Simulation Software)
AIM	Autonomous Intersection Management System
DRL	Deep Reinforcement Learning
MCTS	Monte Carlo Tree Search
QA	Quantum Annealing
QUBO	Quadratic Unconstrained Binary Optimization
MCC	Minimum Clique Cover
AVP	Absolute Value Programming
SSGA	Stop Sign Gap Assist
MPR	Market Penetration Rate
DMPC	Distributed Model Predictive Control
MILP	Mixed Integer Linear Programming
PMILP	Platoon-based MILP
PCC	Predictive Cruise Control
COP	Controlled Optimization of Phases
ASC	Actuated Signal Control
PET	Post-Encroachment Time
TTC	Time-to-Collision
IRS	Integrated Risk Score
GA	Genetic Algorithm

4 Results

This section presents the simulation results, first detailing a single illustrative run to demonstrate the scheduling process and then analyzing the relationship between efficiency gains and intersection complexity across multiple runs.

4.1 Single Run Illustrative Example

To illustrate the simulation logic and the impact of the scheduling and conflict resolution algorithm, a single simulation run was performed for both HDV and CAV scenarios using the parameters specified in Table 2 (next page). Approach A (1) has 3 lanes with 4, 3, and 2 vehicles respectively (total 9), and Approach B (2) has 2 lanes with 3 and 2 vehicles respectively (total 5).

4.1.1 Simulation Parameters

Parameter Justification: The parameters for this specific illustration were chosen to represent distinct operational scenarios and facilitate a clear comparison.

- **HDV Scenario Parameters:** These values represent cautious or typical human driving behavior at a stop-controlled intersection:
  - Speed (v_{HDV}): 66 ft/s ($\approx$ 45 mph), selected as a typical arterial speed limit.
  - Car-Following Headway ($\tau_{F,HDV}$): 4.0 s. This represents cautious driving, falling at the upper end of observed intervals or reflecting conservative assumptions [1].
  - Switching Headway ($\tau_{S,HDV}$): 7.0 s. This value is consistent with typical critical gap ranges (e.g., 6-8 s) cited in HCM methodologies, reflecting the time an HDV driver might need to safely judge gaps [9, 36].
  - Arrival Rate (λ_{HDV}): 0.2 veh/s/approach (720 veh/hr/approach), chosen to represent moderate traffic demand.
  - Deceleration / Acceleration ($a_{min,HDV} = -6$ ft/s^2, $a_{max,HDV} = 5$ ft/s^2): Typical performance values for conventional vehicles.
- **CAV Scenario Parameters:** These values represent efficient, potentially optimistic automated vehicle operation:
  - Speed (v_{CAV}): 81 ft/s ($\approx$ 55 mph), reflecting potentially higher, automated operating speeds.
  - Car-Following Headway ($\tau_{F,CAV}$): 0.8 s. This is a commonly used value in simulation studies for independent (non-platooning) CAVs, consistent with literature discussing sub-second headways (e.g., ranges like 0.6-1.1 s) [11].
  - Switching Headway ($\tau_{S,CAV}$): 1.0 s. This optimistic value was selected specifically to illustrate the high potential efficiency achievable by CAVs in this scenario.
  - Arrival Rate (λ_{CAV}): 0.6 veh/s/approach (2160 veh/hr/approach), chosen to simulate a high traffic demand scenario to test the system under load.
  - Deceleration / Acceleration ($a_{min,CAV} = -12$ ft/s^2, $a_{max,CAV} = 10$ ft/s^2): Represents the potentially higher performance capabilities of CAVs.

Table 2: Parameters for Single Illustrative Simulation Run

Parameter	HDV Scenario Value	CAV Scenario Value
Configuration		
Lanes Approach A ($N_{\text{lanes},1}$)	3	3
Vehicles Approach 1 ($N_{\text{veh},1,l}$)	[4, 3, 2] (Total 9)	[4, 3, 2] (Total 9)
Lanes Approach 2 ($N_{\text{lanes},2}$)	2	2
Vehicles Approach 2 ($N_{\text{veh},2,l}$)	[3, 2] (Total 5)	[3, 2] (Total 5)
Segment Length L (ft)	100	100
Vehicle Length l_{veh} (ft)	14	14
Lane Width w_{lane} (ft)	12	12
Offset $offset$ (ft)	4	4
Operational Parameters		
Arrival Speed v (ft/s)	66	81
Min. Acceleration $a_{\min}$ (ft/s^2)	-6	-12
Max. Acceleration $a_{\max}$ (ft/s^2)	5	10
Arrival Rate λ (1/s)	0.2	0.6
Car-Following Headway τ_F (s)	4.0	0.8
Switching Headway τ_S (s)	7.0	1.0
Derived Parameters		
Traversal Time δ (s)	7.0152	4.6095
Modified $\tau_{F,\text{mod}}$ (s)	4.0	0.8
Modified $\tau_{S,\text{mod}}$ (s)	7.0	1.0
Box Length b_L (ft)	44	44
Box Width b_W (ft)	32	32

In summary, these parameter sets for the illustrative run were carefully selected to create a distinct contrast between plausible cautious HDV operation and efficient CAV operation, allowing for a clear demonstration of the simulation mechanics and potential parameter impacts, informed by ranges found in the cited literature.

4.1.2 Initial Scheduling Results (HDV Scenario - Before Final Adjustments)

The core block-priority scheduling logic first calculates an initial departure sequence based on readiness and initial headway application. Table 3 presents this initial sequence for the HDV scenario, sorted by the initially calculated departure time (t^{+}_{init}). This represents the schedule before the block merging process fully enforces all necessary headway constraints iteratively to eliminate all existing conflicts.

Table 3: HDV Scenario: Initial Scheduling Sequence (Before Conflict Elimination Enforcement)

Approach	Lane	Veh #	Arrival (t^{-})	Potential Stop (t^{0}_{init})	Initial Depart (t^{+}_{init})
1	1	1	5.8182	12.8333	12.8333
2	1	1	5.8182	12.8333	19.8333
1	2	1	17.5936	24.6088	24.6088
1	1	2	11.7754	18.7906	26.8333
2	2	1	19.6429	26.6580	31.6088
1	1	3	24.8294	31.8446	38.6088
2	2	2	29.2201	36.2353	45.6088
1	3	1	42.2839	49.2991	49.2991
1	2	2	30.6476	37.6627	52.6088
1	1	4	48.1021	55.1173	55.1173
2	1	2	35.0383	42.0534	59.6088
2	1	3	55.7400	63.6088	63.6088
1	2	3	36.4658	56.6088	66.6088
1	3	2	57.0081	64.0233	70.6088

4.1.3 Intermediate Vehicle Blocks (HDV Scenario)

The scheduling algorithm identifies groups of vehicles based on approach and timing relative to the $\tau_{S,\text{mod}} = 7.0$ s threshold. The 9 blocks identified for this HDV run, based on the initial schedule, are shown below. Note that stop and departure times within these blocks are still preliminary before the conflict elimination and final merging step.

Block 1 (Size 1): Vehicle A1-1

App	Lane	Veh#	Arrival (s)	Stop (t^{0}_{init})	Depart (t^{+}_{init})
1	1	1	5.8182	12.8333	12.8333

Block 2 (Size 1): Vehicle B1-1

App	Lane	Veh#	Arrival (s)	Stop (t^{0}_{init})	Depart (t^{+}_{init})
2	1	1	5.8182	12.8333	19.8333

Block 3 (Size 2): Vehicles A2-1, A1-2

App	Lane	Veh#	Arrival (s)	Stop (t^0_{init})	Depart (t^+_{init})
1	2	1	17.5936	24.6088	24.6088
1	1	2	11.7754	18.7906	26.8333

Block 4 (Size 1): Vehicle B2-1

App	Lane	Veh#	Arrival (s)	Stop (t^0_{init})	Depart (t^+_{init})
2	2	1	19.6429	26.6580	31.6088

Block 5 (Size 1): Vehicle A1-3

App	Lane	Veh#	Arrival (s)	Stop (t^0_{init})	Depart (t^+_{init})
1	1	3	24.8294	31.8446	38.6088

Block 6 (Size 1): Vehicle B2-2

App	Lane	Veh#	Arrival (s)	Stop (t^0_{init})	Depart (t^+_{init})
2	2	2	29.2201	36.2353	45.6088

Block 7 (Size 3): Vehicles A3-1, A2-2, A1-4

App	Lane	Veh#	Arrival (s)	Stop (t^0_{init})	Depart (t^+_{init})
1	3	1	42.2839	49.2991	49.2991
1	2	2	30.6476	37.6627	52.6088
1	1	4	48.1021	55.1173	55.1173

Block 8 (Size 2): Vehicles B1-2, B1-3

App	Lane	Veh#	Arrival (s)	Stop (t^0_{init})	Depart (t^+_{init})
2	1	2	35.0383	42.0534	59.6088
2	1	3	55.7400	63.6088	63.6088

Block 9 (Size 2): Vehicles A2-3, A3-2

App	Lane	Veh#	Arrival (s)	Stop (t^0_{init})	Depart (t^+_{init})
1	2	3	36.4658	56.6088	66.6088
1	3	2	57.0081	64.0233	70.6088

4.1.4 Scheduling Adjustments (HDV Scenario)

The algorithm then merged these blocks sequentially, applying the $\tau_{S,\text{mod}} = 7.0$ s constraint when the approach switched between blocks, and re-checking the $\tau_{F,\text{mod}} = 4.0$ s constraint within lanes after any shifts. This resulted in adjustments to several vehicles' stop and/or departure times to ensure a conflict-free final sequence that respects the priority order established by the initial block readiness. Examples of adjustments include:

- **Merging Block 6 (Vehicle B2-2):** This block, containing only vehicle B2-2, was merged after Block 5 (whose last vehicle, A1-3, had a final departure $t^+_{final} = 40.8333$ s). The adjustments proceeded as follows:

1. *Apply Switching Headway ($\tau_{S,mod} = 7.0$ s):* Since Block 6 is from Approach B following Block 5 from Approach A, the earliest possible departure for B2-2 is $40.8333 + 7.0 = 47.8333$ s. This is later than its initially calculated departure of 45.61 s.
2. *Check Car-Following Headway ($\tau_{F,mod} = 4.0$ s):* B2-2 follows B2-1 in the same lane (B2-1 had $t^+_{final} = 33.8333$ s after its own adjustments). B2-2's stop time must therefore be no earlier than $33.8333 + 4.0 = 37.8333$ s.
3. *Determine Final Times for B2-2:* The minimum departure time is set by step 1 (47.8333 s). The minimum stop time is set by step 2 (37.8333 s, which is later than its initial potential stop of 36.24 s).
4. *Result:* Final adjusted values for B2-2 are: Stop $t^0_{final} = 37.8333$ s, Departure $t^+_{final} = 47.8333$ s.

- **Merging Block 8 (Vehicles B1-2, B1-3):** This block merged after Block 7 (whose last vehicle, A1-4, departed at $t^+_{final} = 55.1173$ s).
  1. *Apply Switching Headway ($\tau_{S,mod} = 7.0$ s) to First Vehicle (B1-2):* Block 8 (Approach B) follows Block 7 (Approach A). B1-2's departure must be $\geq 55.1173 + 7.0 = 62.1173$ s. This is later than its initial departure of 59.61 s, so its departure is shifted forward.
  2. *Check Car-Following ($\tau_{F,mod} = 4.0$ s) for Second Vehicle (B1-3):* B1-3 follows B1-2 in the same lane. Its stop time must be $\geq$ (B1-2's new departure time 62.1173 s) + $4.0 = 66.1173$ s. This is later than its initial potential stop time of 63.61 s.
  3. *Determine Final Times for Block 8:*
     - B1-2: The departure is set by step 1. Stop $t^0_{final} = 42.05$ s (original potential stop), Departure $t^+_{final} = 62.1173$ s.
     - B1-3: The stop time is set by step 2. Since $t^0_{final} = 66.1173$ s is later than B1-2's departure + $\tau_{F,\text{mod}}$, the departure occurs immediately at the stop time. Stop $t^0_{final} = 66.1173$ s, Departure $t^+_{final} = 66.1173$ s.
- **Merging Block 9 (Vehicles A2-3, A3-2):** Similar logic applied when merging this block after Block 8 (last vehicle B1-3 departed at $t^+_{final} = 66.1173$ s):
  - The $\tau_{S,\text{mod}}$ constraint required the minimum departure for the first vehicle (A2-3 from Approach A) to be $66.1173 + 7.0 = 73.1173$ s.
  - Subsequent checks for $\tau_{F,\text{mod}}$ were performed within Block 9 (between A2-3 and A3-2, and potentially relative to earlier vehicles in their lanes if applicable after shifts) to ensure all headways were satisfied, potentially causing further adjustments to stop/departure times within that block.

These examples illustrate how the block merging process propagates necessary delays to maintain safety headways, particularly after approach switches introduce significant $\tau_{S,\text{mod}}$ delays.

4.1.5 Final Scheduling Results (HDV Scenario After Adjustments)

The final, adjusted sequence of stop (t^0_{final}) and departure (t^+_{final}) times for the HDV scenario, reflecting all adjustments made during block processing, is presented in Table 4. Comparing this table to Table 3 reveals the impact of the conflict resolution process on the timing of nearly every vehicle after the first few. The final calculated efficiency for this HDV run is 15.48%.

Table 4: HDV Scenario: Final Scheduling Results (After Block Processing Adjustments)

Approach	Lane	Veh #	Arrival (t^-)	Final Stop (t^0_{final})	Final Depart (t^+_{final})
1	1	1	5.8182	12.8333	12.8333
2	1	1	5.8182	12.8333	19.8333
1	2	1	17.5936	24.6088	26.8333
1	1	2	11.7754	18.7906	26.8333
2	2	1	19.6429	26.6580	33.8333
1	1	3	24.8294	31.8446	40.8333
2	2	2	29.2201	37.8333	47.8333
1	3	1	42.2839	49.2991	54.8333
1	2	2	30.6476	37.6627	54.8333
1	1	4	48.1021	55.1173	55.1173
2	1	2	35.0383	42.0534	62.1173
2	1	3	55.7400	66.1173	66.1173
1	2	3	36.4658	58.8333	73.1173
1	3	2	57.0081	64.0233	73.1173

In contrast, the simulation output for the CAV scenario (using the same arrival pattern but CAV parameters from Table 2) showed that the initial passing sequence generated by the block-priority logic already satisfied all headway constraints ($\tau_{F,\text{mod}} = 0.8$ s, $\tau_{S,\text{mod}} = 1.0$ s). Therefore, the block merging and re-validation step resulted in no changes to the stop or departure times for the CAVs in this particular run. The final sequence is shown in Table 5. The final efficiency for the CAV scenario was 32.10%, providing an efficiency gain of 107.36%.

Table 5: CAV Scenario: Final Scheduling Results (No Adjustments Needed)

Approach	Lane	Veh #	Arrival (t^-)	Final Stop (t^0_{final})	Final Depart (t^+_{final})
1	3	1	3.6343	8.2438	8.2438
2	2	1	3.6343	8.2438	9.2438
1	2	1	7.2685	11.8781	11.8781
2	2	2	8.2444	12.8540	12.8781
1	1	1	10.9028	15.5123	15.5123
2	1	1	13.4141	18.0237	18.0237
1	2	2	14.5370	19.1466	19.1466
2	1	2	17.0483	21.6579	21.6579
1	3	2	18.1713	22.7809	22.7809
2	1	3	20.6826	25.2922	25.2922
1	1	2	21.8056	26.4151	26.4151
1	2	3	25.4398	30.0494	30.0494
1	1	3	29.0741	33.6836	33.6836
1	1	4	32.7083	37.3179	37.3179

4.1.6 Timeline Visualization

Figure 2 provides a visual representation of the simulation results for the single run example, reflecting the final departure times after all scheduling adjustments. Each panel shows the timeline for either the HDV (left) or CAV (right) scenario. The vertical axis lists the unique identifier for each vehicle (Approach-Lane-Vehicle#, e.g., A1-1 is Approach A or 1, Lane 1, Vehicle 1; B2-1 is Approach B or 2, Lane 2, Vehicle 1), sorted by their final departure time. The horizontal axis represents time in seconds. For each vehicle, markers indicate Arrival (t^-), Stop (t^0_{final}), and Departure (t^+_{final}). The line from Stop to Departure visually represents the delay ($t^+_{\text{final}} - t^0_{\text{final}}$). Annotations provide exact times and the calculated delay. Blue denotes Approach A (1), Red denotes Approach B (2). Comparing the two panels: the CAV timeline (right) is much shorter and seamless ($\approx$ 37 s vs $\approx$ 73 s for HDV) whereas a stop-and-go pattern is noticed often for the HDVs; CAV delays are minimal (average 0.07 s) while HDV delays are significant (average 7.83 s).

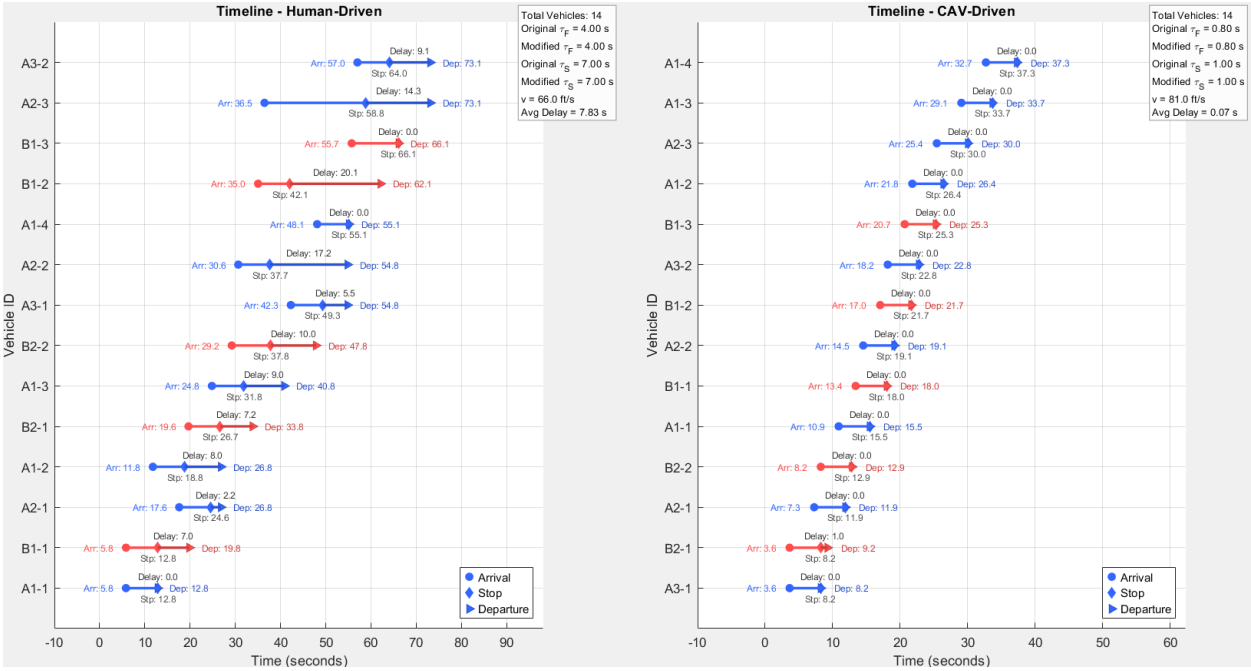

Figure 2: Timeline comparison for the single run illustrative example: Human-Driven (Left) vs. CAV-Driven (Right).

4.1.7 Bird's-Eye View Visualization

Figure 3 shows a snapshot from the animated bird's-eye view comparison at simulation time t = 11.0 s. The left panel depicts the HDV scenario, and the right panel shows the CAV scenario.

Layout: Intersection shown from above. Approach A (horizontal blue dashed lines, Left to Right, lanes A-1 to A-3); Approach B (vertical red dashed lines, Top to Bottom, lanes B-1, B-2); central black dashed box is intersection box including 4 feet offset where vehicles stop at stop line before crossing the intersection.

Vehicles: Blue rectangles are Approach A vehicles, Red are Approach B vehicles. Label 'Xl-i' indicates Approach-Lane-Vehicle#. Time shown is 11.0 s.

Observations at $t = 11.0$ s: In the HDV scenario (Left), vehicles A1-1 and B1-1 are approaching their stop lines. In the CAV scenario (Right), vehicle B2-1 has already departed the intersection and vehicles A1-1, A2-1 and B2-2 are approaching their respective stop lines.

Comparison: This snapshot visually illustrates faster progression in the CAV scenario at the same time point, supporting the efficiency metrics.

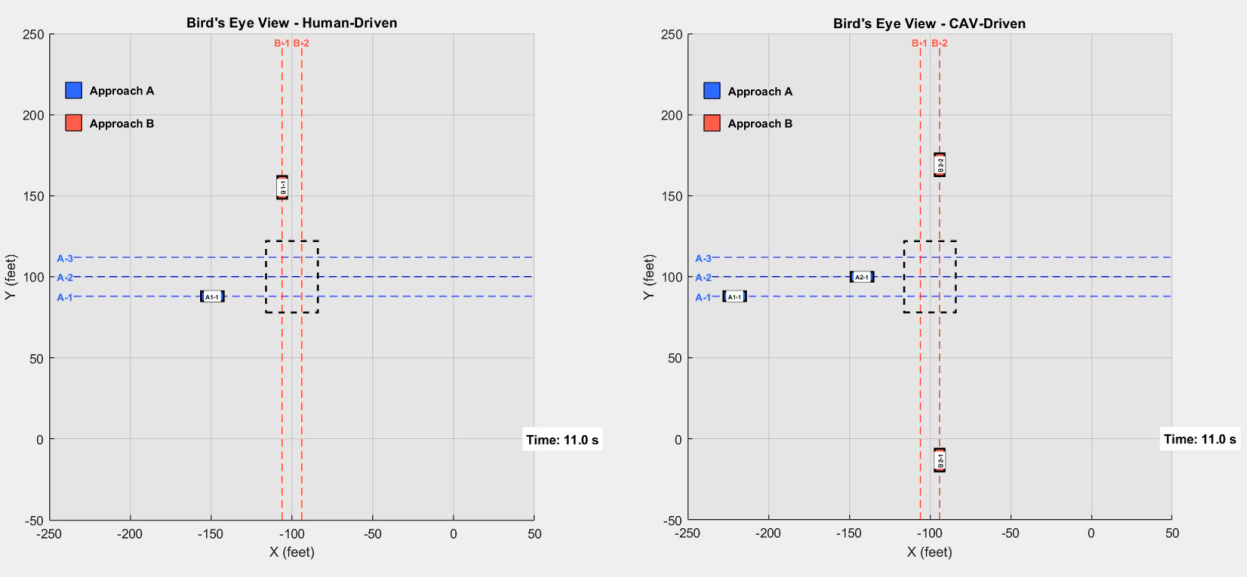

Figure 3: Snapshot of the Bird's Eye View simulation at Time = 11.0 seconds: Human-Driven (Left) vs. CAV-Driven (Right).

4.2 Efficiency Gains vs. Conflict Points

To understand how intersection complexity affects the benefits of CAVs under the simulated block-priority protocol, multiple simulation trials (50,000 for this report) were conducted with varying numbers of lanes (and thus conflict points) and vehicles per lane, using randomized configurations. The percentage gain in throughput efficiency (CAV vs. HDV) was plotted against the number of conflict points ($CP = N_{\text{lanes},A} \times N_{\text{lanes},B}$), as shown in Figure 4. The fixed parameters used for these runs were the default values coded in the second script (HDV: $v = 45$, $\tau_S = 2.5$, $\tau_F = 2$, $\lambda = 0.3$; CAV: $v = 60$, $\tau_S = 0.8$, $\tau_F = 0.6$, $\lambda = 0.7$).

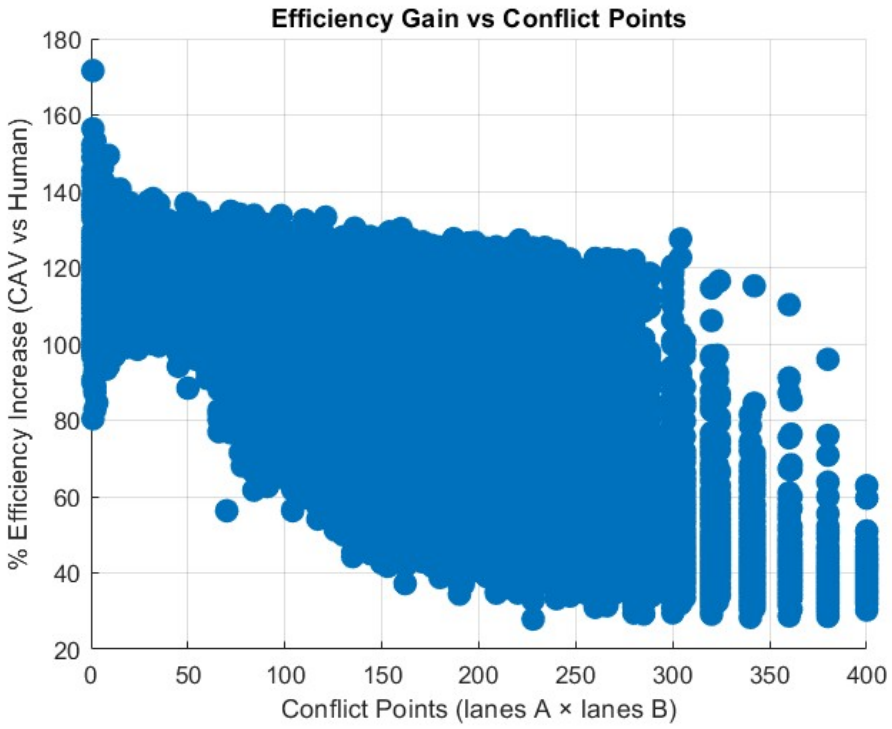

Figure 4: Percentage Efficiency Gain (CAV vs. HDV) as a function of Intersection Conflict Points from 50,000 trials.

4.2.1 Analysis of Trend

Figure 4 shows the percentage efficiency increase when using CAV parameters compared to HDV parameters, plotted against the number of conflict points based on 50,000 trials. Several observations can be made:

- **Universal Positive Gain:** Virtually all 50,000 trials show a positive efficiency gain, indicating that under the assumptions of this model, the CAV parameter set consistently outperforms the HDV set, often substantially (gains range from roughly 25% to over 175%).
- **Peak Gain at Low Complexity:** The highest percentage gains (up to $\approx 175\%$) occur at very low conflict points (CP approx. 1-20). In these simpler configurations (e.g., 1×1, 1×2, 2×1, 2×2 lanes), the intersection operates more like synchronized single channels, where the drastically reduced CAV headways provide the maximum relative advantage over the much larger HDV headways.
- **Decreasing Gain with Increasing Complexity:** A distinct trend emerges where the upper boundary and the central mass of the data points shift downwards as conflict points increase from ≈ 50 towards ≈ 300. This suggests that while CAVs remain more efficient, the *percentage gain* relative to HDVs tends to decrease as the number of conflicting lane pairings increases.
- **Significant Variance:** For any specific number of conflict points, there is a wide spread in the observed efficiency gains. For example, at CP=150, gains vary by almost 100 percentage

points (approx. 40% to 135%). This highlights that the simple conflict point metric is not the sole determinant of efficiency gain.

- **Behavior at Very High Complexity (CP $\geq$ 300):** While data becomes sparser (fewer random trials generated these high lane counts), the downward trend appears to persist or plateau, with most gains clustering below 100%.

Potential explanations for the decreasing gain include the increasing impact of physical clearance time on the minimum switching headway $\tau_{S,\text{mod}}$ at larger intersection sizes (negating some CAV advantage, as the minimum time $(l_{veh} + \max(b_L, b_W))/v$ grows with lane count) and the increased frequency of switching events in more complex scenarios potentially limiting throughput under the block-priority logic. The high variance observed underscores that the efficiency gain depends strongly on other factors beyond just the conflict point count, including specific vehicle counts (traffic volume), the distribution of vehicles across lanes, the arrival rates (λ), the degree of intersection asymmetry (e.g., 1x4 vs 2x2), and the specific stochastic sequence of vehicle arrivals in any given simulation run. These other factors are discussed further in Section 6.

5 Discussion

The simulation results demonstrate quantifiable efficiency gains when replacing HDVs with CAVs, even when both operate under the constraints of a traditional stop-controlled intersection using a rigorously enforced block-priority scheduling protocol. The primary driver for these gains in this model is the difference in operational parameters: CAVs are simulated with potentially higher speeds (v), faster deceleration ($a_{\min}$ influencing δ), shorter car-following headways (τ_F), and shorter switching headways (τ_S).

The detailed single-run analysis (Section 4.1) underscores the necessity of the scheduling algorithm's conflict resolution component. While a simple priority selection based on the earliest ready block provides an initial order, the multi-lane nature introduces conflicts that must be resolved by explicitly enforcing switching headways ($\tau_{S,\text{mod}}$) between blocks from different approaches and propagating the resulting delays, as seen in the adjustments made to the HDV schedule (Table 4). This ensures a safe and physically realistic simulation adhering to the intended priority principle, which is crucial for accurately comparing scenarios. The fact that the CAV scenario in the example did not require adjustments highlights how their inherently faster parameters can sometimes naturally avoid the conflicts that necessitate adjustments for HDVs.

Beyond the single-run illustration, the analysis of efficiency gains versus conflict points (Figure 4) presents a complex picture. While the highest percentage gains are seen at the simplest (1×1) intersections, the general trend suggests a decrease in relative gain as complexity increases, albeit with very high variance.

This implies that while CAV parameters always offer an advantage, factors like the increasing physical clearance time required by larger intersections (impacting minimum $\tau_{S,\text{mod}}$ requirements) might temper this advantage relative to HDVs in more complex configurations under this specific stop-sign protocol. It is crucial to remember that this gain is achieved without leveraging advanced CAV coordination (like reservation systems [37] or optimized scheduling [28, 26, 33]) that could eliminate the need for stopping altogether. The gains observed here represent a baseline improvement achievable solely through enhanced vehicle performance within legacy infrastructure rules.

The comparison highlights that the inherent limitations of human driving (represented by longer headways and potentially slower speeds/reactions in the HDV parameters) significantly constrain

the capacity of stop-controlled intersections.

CAVs, by reducing these limitations, allow for a denser packing of vehicles through the intersection, leading to higher throughput and reduced delays, as evidenced by the efficiency calculations (HDV 15.48% vs CAV 32.10% in the example) and the timeline visualizations (Figure 2, showing a much lower average delay of 0.07 s for CAVs vs 7.83 s for HDVs). However, the magnitude of these gains is directly tied to the specific parameters chosen, as seen in the difference between the illustrative run and the defaults used for the multi-run analysis. More aggressive CAV parameters will naturally yield larger calculated gains. The choice of the theoretical saturation flow rate used in the efficiency calculation also influences the absolute efficiency percentages, although the relative gain between HDV and CAV scenarios remains a robust comparative metric. The assumption of constant departure speed further simplifies the comparison, potentially underestimating the absolute throughput achievable if acceleration were modeled, and also potentially overestimating the required switching headway $\tau_{S,\text{mod}}$. The high variance in the multi-run results emphasizes that factors beyond just the number of conflict points, such as specific arrival patterns and vehicle volumes, significantly impact the realized efficiency gain in any given scenario.

6 Limitations

While the simulation model provides valuable insights, it is important to acknowledge its limitations:

1. **Simplified Geometry:** The model considers only two perpendicular, one-way approaches. Real-world intersections often involve two-way traffic and potentially more than two approaches, significantly increasing complexity.

2. **Traffic Movements:** Only straight-through movements are simulated. Turning movements (left and right turns) introduce additional conflict points and often require different gap acceptance behaviors [3], which are not modeled here. Merging and diverging maneuvers upstream or downstream are also ignored.

3. **Vehicle Dynamics:**

   - Vehicles are assumed to be uniform in size (l_{veh}, w_{veh} based on Table 2). Fleet heterogeneity affects spacing and headways.
   - Arrival speed (v) is assumed constant at the start of segment L.
   - Deceleration is simplified using a constant $a_{\min}$.
   - Crucially, departure is modeled without an acceleration phase; vehicles are assumed to clear the intersection at constant speed v. This is a significant simplification affecting clearance times and efficiency. It makes the model conservative, potentially underestimating throughput. Faster clearance due to acceleration (using a_{max}) could potentially allow for shorter required $\tau_{S,\text{mod}}$.

4. **HDV Model:** The model uses fixed HDV parameters. Real driving involves significant variability (stochasticity) in reaction times, speeds, headways, and gap acceptance. Human errors can lead to longer delays or collisions [19]. The simulation represents a consistent, perhaps "best-case" HDV scenario. Real-world HDV efficiency might be lower, implying larger actual gains from CAVs.

5. **CAV Model:**
    - The model is conservative as it does not explicitly model platooning capabilities like CACC which allow for much shorter intra-platoon headways [11, 19, 4]. $\tau_{F,\text{cav}}$ represents independent CAV following.
    - Perfect sensing and control are implicitly assumed. Delays, noise, or errors are not modeled.
    - Full compliance with the scheduling logic is assumed.
6. **Control Protocol:** Strict adherence to the block-priority stop-sign protocol is assumed. This doesn't capture the full potential of CAVs using cooperative strategies (e.g., reservation-based [7, 37], optimized scheduling [18, 28, 31, 26, 32]) that might deviate from stopping or the specific block-priority rule.
7. **External Factors:** Pedestrians, cyclists, weather, and lighting conditions are not included, which can significantly affect intersection operation and safety.
8. **Conflict Point Realism:** While the multi-trial analysis explored conflict points up to 400 (e.g., 20×20 lanes), such complex configurations are highly unlikely for typical stop-controlled intersections in reality. The trends observed at very high conflict points should be interpreted with caution regarding direct applicability to common stop-sign scenarios.
9. **Headway Adjustment Simplification:** The necessary step of calculating and potentially enforcing minimum physical headways ($\tau_{F,\text{mod}}, \tau_{S,\text{mod}}$) based on vehicle length and intersection dimensions is a safety requirement. However, the subsequent scheduling adjustments that shift entire blocks or re-validate timings represent a specific implementation choice. This block-level adjustment, while ensuring safety and adhering to the protocol, might introduce larger delays than strictly necessary compared to more granular optimization, potentially masking some of the nuanced advantages of CAVs, especially if platooning advantages were considered.
10. **Definition of Complexity:** Using Conflict Points ($N_{\text{lanes},A} \times N_{\text{lanes},B}$) as the sole complexity metric ignores approach asymmetry (e.g., 1×4 vs 2×2). Intersections with the same conflict point count but different lane configurations likely exhibit different operational dynamics, limiting the interpretation of the complexity vs. gain relationship derived solely from this metric.
11. **Factors Influencing Efficiency Gain Variance:** As clearly shown by the scatter in Figure 4, the efficiency gain depends strongly on factors not captured by the conflict points metric alone. These include the specific vehicle counts (traffic volume), the distribution of vehicles across lanes, the arrival rates (λ), the degree of intersection asymmetry, and the specific stochastic sequence of vehicle arrivals in any given simulation run. Conclusions drawn solely based on the conflict points trend must acknowledge these other significant influences.

7 Conclusion

This study quantified the potential efficiency gains at multi-lane, stop-controlled intersections resulting purely from the enhanced operational parameters of Connected and Automated Vehicles (CAVs) compared to Human-driven Vehicles (HDVs), using a consistent, block-priority scheduling protocol simulated in MATLAB with explicit multi-lane conflict resolution. The key findings are:

1. **Significant Efficiency Gains:** Replacing HDVs with CAVs, characterized by shorter headways (τ_F, τ_S), potentially higher speeds (v), and faster deceleration (a_{min}), leads to substantial increases in intersection throughput efficiency (e.g., from 15.48% to 32.10% in the illustrative example) and reductions in average vehicle delay, even without advanced cooperative control strategies and despite conservative assumptions like no departure acceleration.

2. **Conflict Resolution is Necessary:** Accurate modeling of multi-lane stop-controlled intersections under group-based priority requires careful enforcement of switching ($\tau_{S,\text{mod}}$) and car-following ($\tau_{F,\text{mod}}$) headways during the scheduling process to resolve conflicts and ensure safety.

3. **Impact of Complexity:** The relative efficiency gain offered by CAVs shows a complex relationship with the number of intersection conflict points, generally decreasing from a peak at low complexity but exhibiting high variance. This suggests that while CAV parameter advantages persist, factors like increasing physical clearance time and other stochastic elements significantly influence the outcome.

4. **Parameter Sensitivity:** The magnitude of the observed gains is directly dependent on the specific performance parameters assumed for both HDV and CAV scenarios.

The major takeaway is that improved vehicle characteristics inherent to CAVs can provide considerable benefits at legacy intersections, forming a baseline improvement upon which more advanced coordination strategies can build. However, the realized gain is highly variable and depends on numerous factors beyond just intersection complexity (including vehicle counts, arrival rates, lane distributions, asymmetry, and stochasticity, as noted in Section 6). This work highlights the inefficiency imposed by human driver limitations and the potential for automation to alleviate these constraints, while also providing a validated simulation tool for further investigation. The MATLAB code developed for this simulation study is available for review and further research on GitHub [12].

8 Practical Recommendations, Implications and Future Work

Practical Recommendations and Implications

The findings of this simulation study, while based on specific models and assumptions, suggest several practical recommendations for stakeholders involved in traffic management and CAV development:

1. **Leverage Baseline CAV Capabilities:** Traffic management agencies should recognize that significant efficiency improvements (as quantified in Section 4) can be realized at existing stop-controlled intersections simply by allowing CAVs to operate using their inherent capabilities (e.g., safely reduced headways), even before full cooperative intersection management systems are deployed. Policies could explore facilitating this as CAV penetration increases, potentially viewing it as an incremental step towards smarter infrastructure.

2. **Account for Geometric Constraints in CAV Design:** CAV developers and standards organizations should consider the impact of physical intersection size on optimal operational parameters. While CAVs can achieve very short electronic headways, the simulation shows physical clearance times can become the bottleneck for switching headways ($\tau_{S,\text{mod}}$) in larger, multi-lane intersections (as discussed regarding Figure 4). CAV control logic could potentially

adapt desired headways based on detected or mapped intersection geometry, or prioritize strategies like efficient intra-approach platooning where switching penalties are frequent.

3. **Emphasize Site-Specific Analysis:** Given the high variance in efficiency gains observed at similar complexity levels (Figure 4), traffic engineers should perform detailed, site-specific simulations (using models that capture multi-lane interactions) when evaluating potential CAV impacts or planning modifications for specific stop-controlled intersections. Relying solely on aggregate metrics like conflict points or average parameter benefits may not provide accurate predictions for a particular location, as efficiency gains depend heavily on local factors like lane configurations, arrival patterns, and traffic volumes (see Section 6).

4. **Factor in Departure Acceleration:** Future performance evaluations and potential control strategy designs for CAVs at stop-controlled intersections should incorporate realistic departure acceleration (a_{max}). This study's conservative assumption of constant departure speed likely underestimates achievable throughput (as noted in Section 6). Accounting for acceleration could reveal even greater efficiency benefits and potentially allow for adjustments to required switching headways ($\tau_{S,\text{mod}}$).

5. **Promote V2X for Enhanced Benefits:** While this study shows gains from CAV parameters alone under the block-priority protocol, realizing the *full* potential of CAVs at intersections likely requires cooperative strategies (platooning, reservation systems, optimized scheduling, etc.). Therefore, continued investment in Vehicle-to-Everything (V2X) communication infrastructure and the development/adoption of interoperable standards for cooperative driving remain crucial for maximizing future benefits at all intersection types, including traditionally unsignalized ones.

Integrating these considerations can help guide the transition towards mixed and fully automated traffic environments more effectively.

Future Work

Based on the study's limitations, several avenues for future research are apparent:

1. **Enhance Realism:**
   - Incorporate realistic acceleration profiles (utilizing a_{max}) for vehicles departing the intersection. This would provide less conservative efficiency estimates and allow investigation into how faster clearance affects minimum required $\tau_{S,\text{mod}}$.
   - Model heterogeneous vehicle types.
   - Introduce stochasticity into HDV behavior (e.g., variable gap acceptance [3]).
   - Include turning movements [37].
   - Expand to two-way traffic and complex geometries.
   - Add external factors like pedestrians/cyclists.
2. **Advanced CAV Modeling:**
   - Implement Cooperative Adaptive Cruise Control (CACC) models [19] to simulate CAV platooning explicitly [4].

- Explore and simulate alternative CAV intersection control strategies (e.g., reservation-based [7], optimization-based [28, 31], game-theoretic [15, 38], learning-based [33, 24]). Investigate optimized deviations from the block-priority logic.
- Investigate impact of communication imperfections (delay, packet loss).
- Refine headway management beyond simple overwriting/block shifts.
- Consider distributed control frameworks [25].

3. **Broader Scope:**

- Extend analysis to other intersection types (signalized, roundabouts) [35].
- Investigate network-level impacts [33].
- Conduct sensitivity analyses on wider range of parameters (arrival rates, volumes, mix ratios [19, 21]).
- Incorporate more nuanced complexity metrics, explicitly studying asymmetry (e.g., 1x4 vs 2x2).
- Validate simulation findings against real-world data or more detailed driving simulator studies [21].

Addressing these areas will provide a more comprehensive understanding of CAV impacts on intersection performance and inform the development of effective traffic management strategies for the future mixed-fleet environment.

A References

References

[1] K. Aghabayk, M. Sarvi, and W. Young, "A Study on Following Behavior Based on the Time Headway," *Jurnal Kejuruteraan*, vol. 32, no. 2, pp. 187-196, Apr. 2020.

[2] A. Ahmad, A. S. Al-Sumaiti, Y.-J. Byon, and K. Al Hosani, "Eco-Driving Framework for Autonomous Vehicles at Signalized Intersection in Mixed-Traffic Environment," *IEEE Access*, vol. 12, pp. 85291-85307, 2024. doi: 10.1109/ACCESS.2024.3415495.

[3] M. Arafat, M. Hadi, T. Hunsanon, and K. Amine, "Stop Sign Gap Assist Application in a Connected Vehicle Simulation Environment," *Transportation Research Record: Journal of the Transportation Research Board*, vol. 2675, no. 9, pp. 1127-1135, Sep. 2021. doi: 10.1177/03611981211006111.

[4] C. Chen, M. Cai, J. Wang, K. Li, Q. Xu, J. Wang, and K. Li, "Multi-Lane Unsignalized Intersection Cooperation Strategy Considering Platoons Formation in a Mixed Connected Automated Vehicles and Connected Human-Driven Vehicles Environment," *IEEE Transactions on Vehicular Technology*, vol. 71, no. 11, pp. 11351-11366, Nov. 2022. doi: 10.1109/TVT.2022.3196434. (Based on abstract/metadata)

[5] D. Chen, S. Ahn, M. Chitturi, and D. A. Noyce, "Towards vehicle automation: Roadway capacity formulation for traffic mixed with regular and automated vehicles," *Transportation Research Part B: Methodological*, vol. 100, pp. 196–221, Jun. 2017.

[6] Clark County Public Works, "Information on Traffic Control Devices." [Online]. Available: https://www.clarkcountynv.gov/public-works/traffic-management/Documents/UnwarrantedTrafficControl.pdf

[7] Dresner, K., & Stone, P. (2008). A multiagent approach to autonomous intersection management. *Journal of Artificial Intelligence Research*, 31, 591-656.

[8] U.S. Department of Transportation, Federal Highway Administration. (2017). *Traffic Congestion and Reliability: Trends and Advanced Strategies for Congestion Mitigation.* Report No. FHWA-HOP-17-XXX. Washington, D.C.

[9] U.S. Department of Transportation, Federal Highway Administration. "Appendix N: Procedures for Estimating Highway Capacity." *HPMS Field Manual.* [Online]. Available: https://www.fhwa.dot.gov/ohim/hpmsmanl/appn6.cfm

[10] D. Gao, "Car-following coordination method based on reinforcement learning for intelligent connected vehicles," in *Proc. SPIE 12645, International Conference on Computer, Artificial Intelligence, and Control Engineering (CAICE 2023)*, 126452D, May 2023. doi: 10.1117/12.2681269. (Based on abstract)

[11] A. Ghiasi, O. Hussain, Z. Qian, and X. Li, "A Mixed Traffic Capacity Analysis and Lane Management Model for Connected Automated Vehicles: A Markov Chain Method," *Transportation Research Part B: Methodological*, vol. 106, pp. 267-291, Dec. 2017.

[12] A. Roy Malakar. (2025). *cav-stop-intersection-simulation* [MATLAB Simulation Code link]. GitHub. Available at https://github.com/arm-nix/cav-stop-intersection-simulation

[13] Y. Gu, L. Wang, L. Cheng, and G. Gu, "An IoT-Based Framework for Motion Planning of Connected Automated Vehicles at Signal-Free Traffic Intersections," *IEEE Internet of Things Journal*, vol. 11, no. 22, pp. 35752-35761, Nov. 2024. doi: 10.1109/JIOT.2023.3337298. (Based on abstract)

[14] Y. Guo and J. Ma, "DRL-TP3: A learning and control framework for signalized intersections with mixed connected automated traffic," *Transportation Research Part C: Emerging Technologies*, vol. 132, p. 103416, Nov. 2021. doi: 10.1016/j.trc.2021.103416.

[15] P. Hang, C. Huang, Z. Hu, and C. Lv, "A Game-Theoretic Approach on Conflict Resolution of Autonomous Vehicles at Unsignalized Intersections," *IEEE Transactions on Intelligent Vehicles*, vol. 8, no. 3, pp. 2077-2088, Mar. 2023. doi: 10.1109/TIV.2022.3232976. (Based on abstract/metadata)

[16] INRIX. (2019). *INRIX 2019 Global Traffic Scorecard.* Kirkland, WA: INRIX.

[17] Jiang, H., Hu, J., An, S., Wang, M., & Park, B. B. (2017). Eco approaching at an isolated signalized intersection under partially connected and automated vehicles environment. *Transportation Research Part C: Emerging Technologies*, 85, 396-411.

[18] Q. Jin, G. Wu, K. Boriboonsomsin, and M. Barth, "Multi-Agent Intersection Management for Connected Vehicles using an Optimal Scheduling Approach," in *2012 International Conference on Connected Vehicles and Expo (ICCVE)*, Beijing, China, Dec. 2012, pp. 185-190. doi: 10.1109/ICCVE.2012.41.

[19] A. Karbasi and S. O'Hern, "Investigating the Impact of Connected and Automated Vehicles on Signalized and Unsignalized Intersections Safety in Mixed Traffic," *Future Transportation*, vol. 2, no. 1, pp. 24-40, Jan. 2022. doi: 10.3390/futuretransp2010002.

[20] A. Karbasi, M. Vafaei, and S. O'Hern, "Investigating the effect of Automated Vehicles and Connected and Automated Vehicles on the capacity of freeways using microscopic simulation (in Persian)," *Civil Engineering Infrastructures Journal*, vol. 54, no. 2, pp. 331-346, Dec. 2021. doi: 10.22059/CEIJ.2021.317910.1734. (Based on abstract)

[21] S. Lee, Y. Jo, A. Jung, J. Park, and C. Oh, "Evaluation of automated driving safety in urban mixed traffic environments," *IET Intelligent Transport Systems*, vol. 18, Suppl. 1, pp. 2963-2976, 2024. doi: 10.1049/itr2.12602.

[22] Levin, M. W., Boyles, S. D., & Patel, R. (2016). Paradoxes of reservation-based intersection controls in traffic networks. *Transportation Research Part A: Policy and Practice*, 90, 14-25.

[23] L. Li, J. Gan, F. Yang, B. Ran, and J. Zhang, "A Method to Calculate the Capacity of Unsignalized Intersection for Connected and Automated Vehicles Based on Gap Acceptance Theory," in *CICTP 2019: Transportation in China—Connecting the World*, Nanjing, China, Jul. 2019, pp. 5600-5612. doi: 10.1061/9780784482292.482.

[24] X. Li, X. Su, J. Wang, and J. Wang, "Discrete Platoon Control at an Unsignalized Intersection Based on Q-learning Model," *Automotive Engineering*, vol. 44, no. 9, pp. 1318-1324, 2022. doi: 10.19562/j.chinasae.qcgc.2022.09.009. (Based on abstract)

[25] C. Liu, C. Lin, and S. G. Anavatti, "Distributed conflict resolution for connected autonomous vehicles," *IEEE Access*, vol. 6, pp. 31307-31315, 2018. doi: 10.1109/ACCESS.2018.2842252. (Based on abstract/metadata)

[26] S. Liu et al., "Coordination of Connected and Automated Vehicles at Unsignalized Intersections Using Hybrid Quantum Annealing," in *2024 IEEE International Conference on Unmanned Systems (ICUS)*, Wuhan, China, Mar. 2024, pp. 1460-1467. doi: 10.1109/ICUS61736.2024.10840144.

[27] H. Liu, K. Niu, H. Wang, Z. Zhang, A. Song, and Z. Wu, "Research on Speed Guidance Strategies for Mixed Traffic Flow Considering Uncertainty of Leading Vehicles at Signalized Intersections," *Applied Sciences*, vol. 14, no. 18, p. 8161, Sep. 2024. doi: 10.3390/app14188161.

[28] Z. Lu, T. Wu, J. Su, Y. Xu, B. Qian, T. Zhang, and H. Zhou, "Toward edge-computing-enabled collision-free scheduling management for autonomous vehicles at unsignalized intersections," *Digital Communications and Networks*, vol. 10, no. 3, Part 1, pp. 1600-1610, Mar. 2024. doi: 10.1016/j.dcan.2024.03.001.

[29] D. Lv, Q. Wuniri, W. Chu, H. Yu, and X. Du, "A priority tree based coordination method for intelligent and connected vehicles at unsignalized intersections," *IET Intelligent Transport Systems*, vol. 15, no. 8, pp. 1053-1063, Aug. 2021. doi: 10.1049/itr2.12082.

[30] Concepts adapted from CIVENGR 570: Connected and Automated Transportation Systems, University of Wisconsin-Madison, Spring 2025 (Instructor: Prof. Xiaopeng Li).

[31] X. Pan, B. Chen, S. A. Evangelou, and S. Timotheou, "A Convex Optimal Control Framework for Autonomous Vehicle Intersection Crossing," *IEEE Transactions on Control Systems Technology*, vol. 31, no. 5, pp. 2011-2026, Sep. 2023. doi: 10.1109/TCST.2022.3226321. (Based on abstract/metadata)

[32] C. Shao, H. Feng, H. Liu, K. Lai, and M. Cen, "Passing method at unsignalized intersections for intelligent vehicle," in *2023 35th Chinese Control and Decision Conference (CCDC)*, Yichang, China, 2023, pp. 200-206. doi: 10.1109/CCDC58219.2023.10326783.

[33] Y. Shi, W. Wang, X. Tao, I. Dusparic, and V. Cahill, "Applying Neural Monte Carlo Tree Search to Unsignalized Multi-intersection Scheduling for Autonomous Vehicles," in *2024 IEEE/RSJ International Conference on Intelligent Robots and Systems (IROS)*, Abu Dhabi, UAE, Oct. 2024, pp. 935-942. doi: 10.1109/IROS58592.2024.10801887.

[34] A. B. N. A. M. Soomro, H. M. Saim, and H. Malik, "Smart road management system for prioritized autonomous vehicles under vehicle-to-everything (V2X) communication," *Multimedia Tools and Applications*, vol. 83, pp. 41637-41654, Oct. 2023. doi: 10.1007/s11042-023-16950-1.

[35] P. Tafidis, A. Pirdavani, T. Brijs, and H. Farah, "Intersection Control Type Effect on Automated Vehicle Operation," in *CICTP 2019: Transportation in China—Connecting the World*, Nanjing, China, Jul. 2019, pp. 2742-2750. doi: 10.1061/9780784482292.238.

[36] K. FitzPatrick, "Gaps Accepted at Stop-Controlled Intersections," *Transportation Research Record*, no. 1303, pp. 103-112, 1991.

[37] I. Tunc, A. Y. Yesilyurt, Z. Gumus, K. Sert, A. O. Koroglu, and M. T. Soylemez, "A platoon ordering algorithm on reservation based intersection management systems," *Alexandria Engineering Journal*, vol. 88, pp. 36-44, Jan. 2024. doi: 10.1016/j.aej.2023.12.064.

[38] W. Wei, S. Wang, W. Ma, and X. Jiang, "Cooperative Game Approach for Conflict Resolution at Unsignalized Intersections among Autonomous Vehicles," *Sustainability*, vol. 14, no. 7, p. 3838, Mar. 2022. doi: 10.3390/su14073838.

[39] M. Zhu, X. Wang, S. D. H. Valeria, H. Guo, M. McDonald, and B. H. Park, "Car-Following Headways in Different Driving Situations: A Naturalistic Driving Study," in *CICTP 2016: Green and Multimodal Transportation and Logistics*, Shanghai, China, Jul. 2016, pp. 1418-1429. doi: 10.1061/9780784479896.120.

[40] Y. Zou, F. Zheng, C. Liu, and X. Liu, "Integrated optimization of traffic signals and vehicle trajectories for mixed traffic at signalized intersections: A two-level hierarchical control framework," *Transportation Research Part C: Emerging Technologies*, vol. 169, p. 104884, Dec. 2024. doi: 10.1016/j.trc.2024.104884.

[41] American Association of State Highway and Transportation Officials (AASHTO), *A Policy on Geometric Design of Highways and Streets*, 7th ed. Washington, D.C.: AASHTO, 2018.

[42] Volkswagen AG, *2017 Golf Technical Specifications* https://media.vw.com/assets/documents/original/6414-197243143857d84873ee336.pdf (Technical Specification Data), circa 2017.